Heat Transfer from Corotating and Stationary Parallel Concentric Disks with Internal Heat Generation

Biswajit Banerjee
Research Scholar
K. V. Chalapathi Rao
Assistant Professor
V. M. K. Sastri
Professor and Head
Department of Mechanical Engineering, Indian Institute of Technology, Madras, India

■Experimental investigations are carried out for the determination of heat transfer coefficients between corotating and stationary parallel disks with internal heat generation. The model considered simulates a typical induction motor with unequal losses in the stator and rotor. The data collected cover a range of Reynolds and Taylor numbers for various heat inputs. Quantitative assessment has been made for the increase in heat transfer with speed of rotation and coolant flow, air being the cooling medium. Temperatures along the axial, radial, and tangential directions are measured, and heat transfer coefficients at the radially diverging section are evaluated. The results are especially relevant to the thermal design of electric machines, and more particularly to radially ventilated induction motors. The results obtained indicate that present-day designs are conservative and that considerable saving in material can be achieved.

Keywords: *augmentation, forced convection, heat generation, rotating flows*

INTRODUCTION

Optimal thermal design of a rotating electric machine is a subject of interest for both electrical and mechanical engineers. The determination of the exact distribution of various losses that occur in an electric machine and the method and extent of their dissipation have a direct bearing on the size of the machine. In order to predict the cooling effectiveness in the machine, a knowledge of heat transfer coefficients in the coolant duct passages as well as the thermophysical properties of the fluid is essential. Almost all designs adopt values of the heat transfer coefficient applicable to simple geometries under stationary conditions, which lead to conservative designs and consequently result in wastage of material [1, 2].

Classical work on heat transfer from rotating disks falls into four main categories: (1) disk rotating without enclosure; (2) disk rotating in an enclosure; (3) parallel disks, with one disk rotating and the other stationary with source or sink flow; (4) corotating parallel disks with different boundary conditions.

Airflow in rotating systems is quite complex, and one has to consider the centrifugal forces as well as the Coriolis forces in addition to the boundary-layer effects and stability criteria. Convective heat transfer is related to flow characteristics and hence is equally complex.

Several investigators have reported both analytical and experimental work. Subba Rao [3] experimentally investigated heat transfer from partially enclosed disks rotating in air with uniform heat flux in the range of local Re ~ 10^4–10^6, spacing ratio ~ 0.01–0.17, and sink flow ~ 0–62.6 kg/h. He proposed empirical relations for predicting local heat transfer coefficients. Mochizuki et al [4] analyzed the heat transfer mechanisms and performance in multiple parallel disk assemblies. They considered the enhancement in the four flow regimes, namely, pure laminar, laminar-oscillating-laminar, laminar-oscillating-turbulent-laminar, and laminar-oscillating-turbulent type convection. Further they investigated the disk spacing, size, and influx disturbance. They analyzed the slug flow and Poiseuille flow conditions and concluded that the disk device had performance characteristics comparable to a high-performance plate-fin compact surface. Sim and Yang [5] studied numerically the heat transfer in laminar flow through corotating parallel disks. A theoretical model was developed to determine the heat transfer performance in laminar flow through a pair of corotating parallel disks. The flow was assumed to enter at the center from both sides and proceed radially outward. A finite difference scheme was employed to obtain numerical results. The effects of rotational number, through-flow Reynolds number (Re), Prandtl number (Pr), and system geometry on heat transfer performance were determined.

Kreith [6] simplified the Navier-Stokes equations for laminar source flow between two corotating parallel disks and obtained solutions by series expansion. Average Nusselt numbers were evaluated numerically for several boundary conditions as a function of Re, Pr, and Taylor number (Ta). For zero rotational speed, the analysis showed good agreement with his experimental work. In the turbulent flow region, an empirical equation for the Nusselt number (Nu) at zero rotation was obtained from experimental data, and a method for evaluating the average Nusselt number in the mixed flow regime was proposed. It is apparent from the literature that no significant work was done to determine the heat transfer

Address correspondence to Dr. K. V. Chalapathi Rao, Assistant Professor, Department of Mechanical Engineering, IIT, Madras 600 036, India.

Experimental Thermal and Fluid Science 1988; 1:195–206

0894-1777/88/$3.50

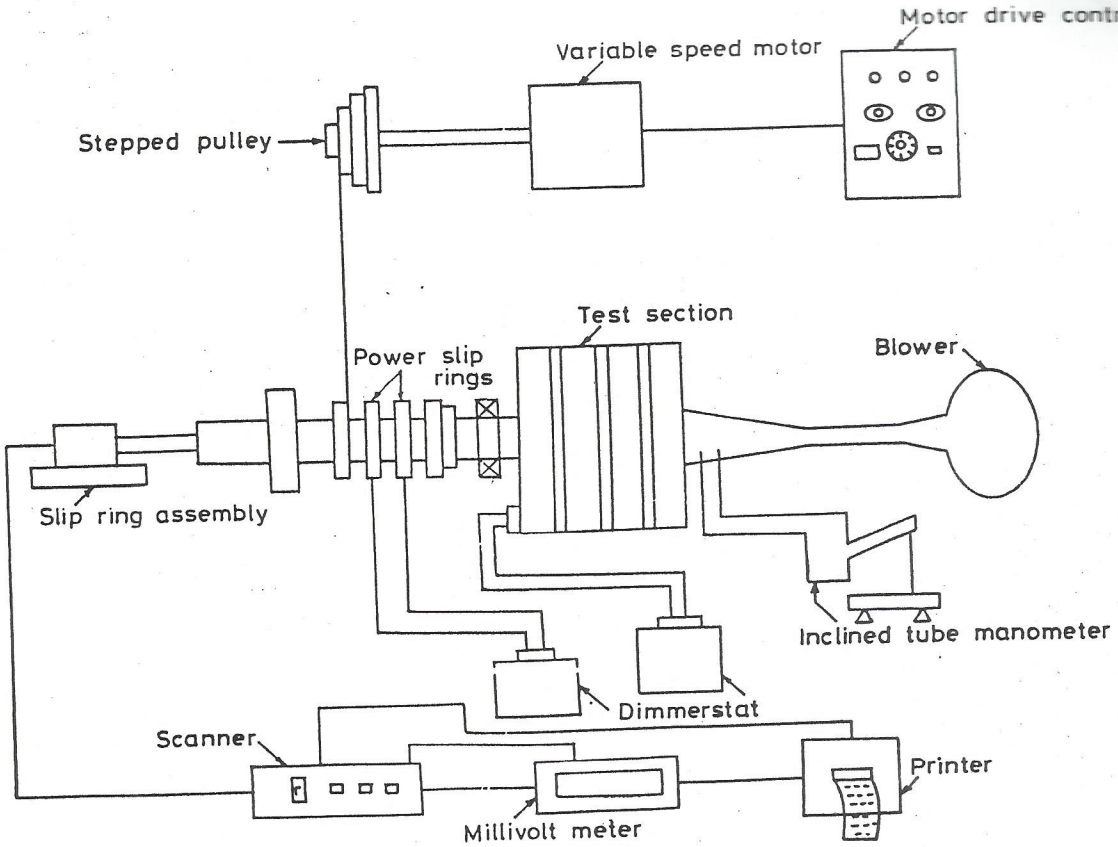

Figure 1. General layout for the setup.

coefficients from corotating radial passages, the data for which are vital to the design of radially ventilated electric machines.

In the present work an attempt is made to simulate geometrically the rotor and stator of a 600 kW induction motor with radial ventilating channels.

EXPERIMENTAL SETUP

The general layout of the experimental setup is shown in Fig. 1. The setup is designed to study the heat transfer from the surfaces of the stator and rotor disks to air, which is the cooling medium. A sectional view of the test section is shown in Fig. 2. Air enters the test section through the annulus formed between the rotor shaft and the rotor disks (hereinafter referred to as the rotor annulus).

The details of the rotor assembly are shown in Fig. 2. Four mild steel disks of 293 mm O.D., 167.5 mm I.D., and 20 mm thickness constitute the rotor test section. Two end flanges, screwed to the rotor shaft, hold the disks by means of through-bolts.

The rotor shaft is provided with steps at either end to accommodate two insulating disks to minimize axial conduction. The shaft is made hollow to provide space for taking out the rotor thermocouple wires and the power cables for the rotor heaters. While these wires and cables come out at the opening on the left through a hole in the insulating disk, the opening on the right is closed by a similar insulating disk. Resistance heaters are employed to simulate the heat generation in the electric machine.

To facilitate insertion of heaters, 12 slots are cut circumferentially in each rotor disk. Each slot measures 28 mm × 5 mm. The rotor assembly is thus considered to simulate the conditions of a rotor in an actual electric machine.

The stator, also shown in Fig. 2, is also made of mild steel and consists of four disks of 430 mm O.D., 295 mm I.D., and 20 mm thickness. The disks are held to stator end flanges in the same manner as those for the rotor disks. The end flanges rest on two ball bearings mounted on the rotor shaft with the inner race rotating. When the stator is mounted with proper supports, it is concentric with the rotor, providing a rotor-stator air gap of 1 mm. Nine slots 36 mm × 7.5 mm are cut circumferentially in each stator disk for insertion of stator heaters. All eight disks and four end flanges are chrome-plated to prevent the formation of rust and thereby maintain a clean surface.

Mild steel rings, 5 mm thick, are used as spacers and are placed between each disk of the rotor and stator assemblies over the through-bolts. Thus a continuously diverging radial duct of 5 mm width, through which the coolant flows, is formed between the disks.

An end shaft (Fig. 3), connected to the left of the rotor shaft holds the pulley for the rotor drive, a power slip ring for the rotor heater, and a Hylam disk, which connects the rotor thermocouples to the slip-ring assembly.

An O-ring is inserted along the circumferential groove in

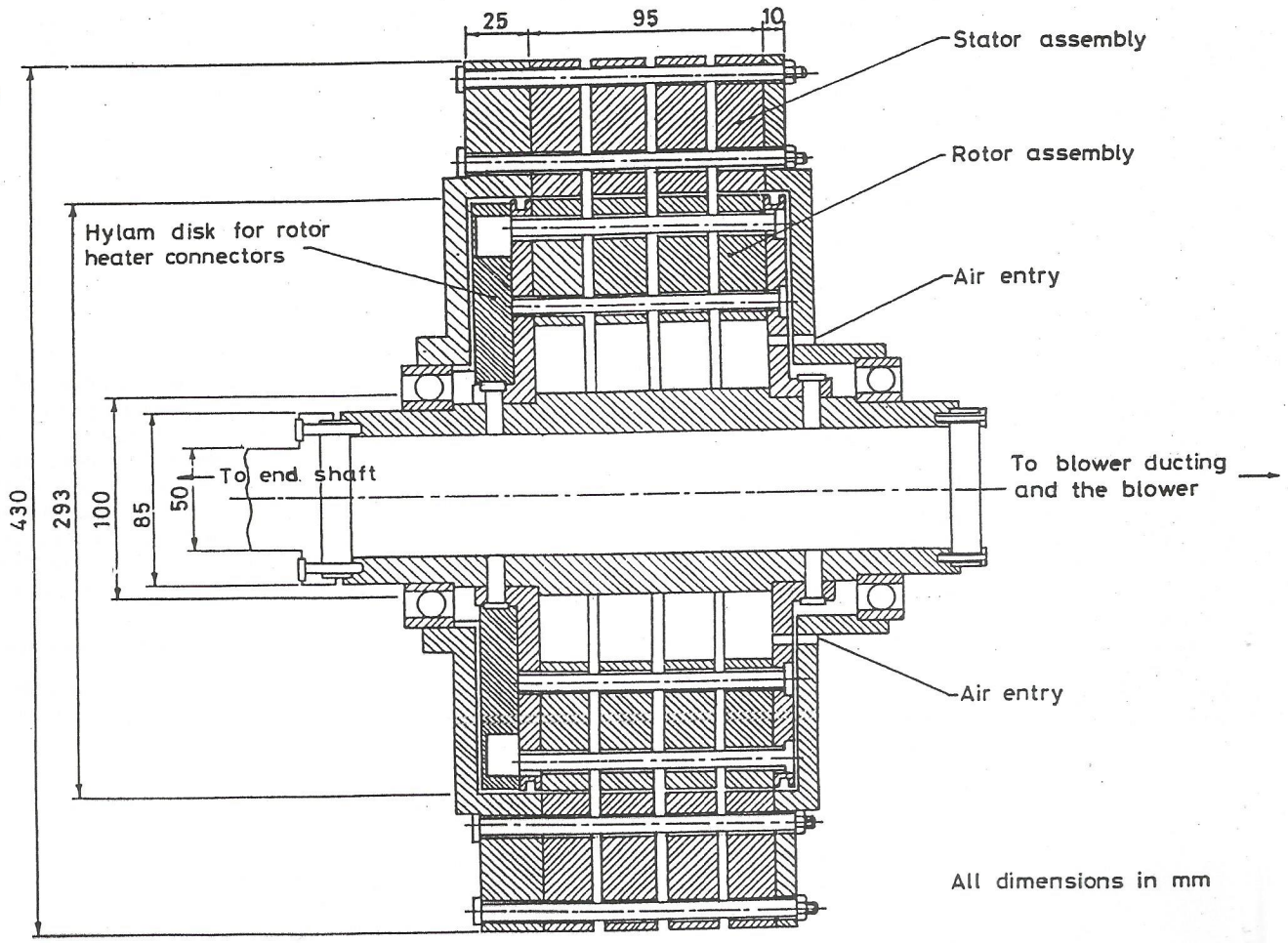

Figure 2. Sectional view of the test section.

each end flange of the rotor. The O-rings project out of the grooves to the extent that they just do not touch the stator end flanges but prevent leakage of air in the axial direction. Also, the holes in the stator and rotor end flanges through which the heater lead wires are taken out are filled with suitable packing material to prevent leakage of air.

A Hylam disk is fixed over the left end flange of the rotor. The inner face of the disk has a circumferential groove deep enough to house the porcelain connectors to which the rotor heaters are connected. Lead wires from each heater are connected to a porcelain connector, and power is supplied to them in parallel.

The Drive Mechanism

The rotor is driven by a variable-speed motor through a pulley and belt drive. Stepped pulleys are used to get different speeds. A rectifier unit controls the speed of the dc motor. The arrangement allows attainment of rotor speeds up to 1500 rpm.

The Coolant Flow Circuit

The coolant used is air, and its flow path is shown in Fig. 4. The air required for the test is obtained from a centrifugal blower, and the actual flow rates of the coolant air in the test section range from 1.3×10^{-2} to 2.7×10^{-2} kg/s. The air is uniformly admitted all over the rotor annulus through the circular openings in the stator and rotor end flanges on the right. Then it enters the radial ducts of the rotor and stator and finally comes out at the back of the stator disks. The exhaust air is let off to the atmosphere.

The Test Section

The four pairs of stator and rotor disks, when assembled, form three diverging radial ducts of equal dimensions between them. As already mentioned, the coolant air finds its way through these ducts from the rotor annulus. Axial flow of air in the rotor-stator air gap is not considered. Of the three radial ducts, the central duct constitutes the test passage.

Heater Assembly

The heating elements are rectangular and have nichrome coils inserted in them. The coils, wrapped over mica sheets, are insulated from the steel housing by more layers of mica. The maximum heating capacities of the stator and rotor heaters, which extend from one end of the test section to the other, are

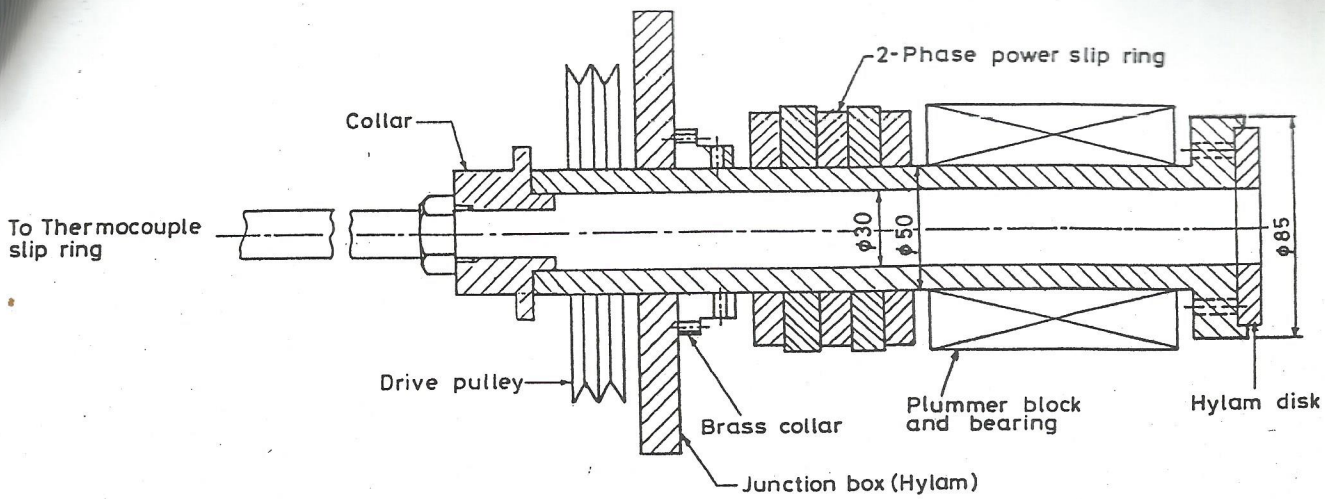

Figure 3. Left endshaft.

125 W and 80 W, respectively. Much care is taken to properly insulate the lead wires that exit the heaters through small holes drilled in the steel enclosure. The heaters are then inserted into the axial slots in the rotor and stator, ensuring good contact between the disk surface and the heater housings. The heaters thus simulate the heat generation by the conductors in a rotating electric machine.

The heat generation in the disks is varied from 300 to 1000 W in the rotor and stator.

Measurement of Temperature

Double-insulated copper-constantan thermocouples are fixed on both sides of the two inner disks of the stator and rotor assembly. Thermocouples are also placed in the air spaces of the central radial duct. The locations of these thermocouples are shown in Figs. 5 and 6. Nine thermocouples are fixed on the stator disk surfaces facing the central duct, whereas five thermocouples are fixed to each of the other faces. For the rotor, five thermocouples are fixed on the disk surfaces facing the central duct and four on each of the other faces. For measurement of air temperature in the radial duct, two thermocouples are located in the stator duct and two in the rotor duct at convenient locations. Thermocouple beads are made in an inert atmosphere to prevent any formation of oxides. Radial grooves are milled on the disks to seat the thermocouples. The grooves are such that after they are fixed the thermocouples are flush with the surface. At the point of

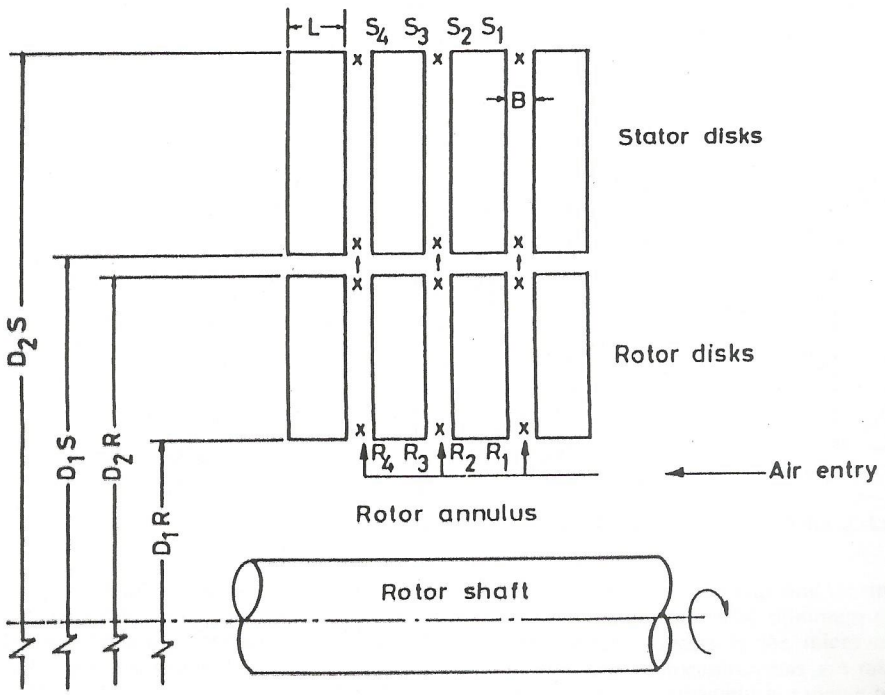

Figure 4. Numbering of stator and rotor disks for thermocouple locations. X marks air thermocouple locations; arrows indicate the airflow path.

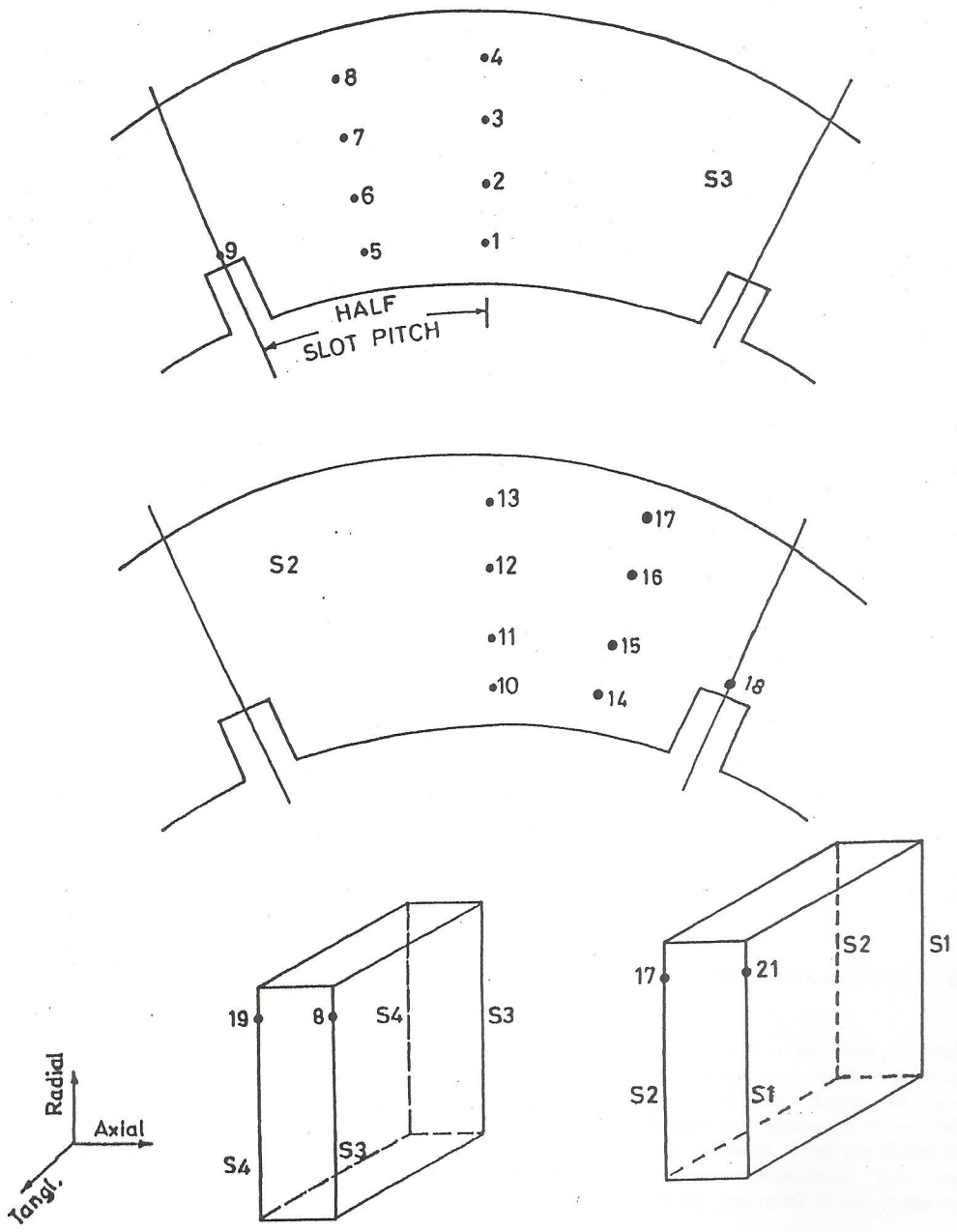

Figure 5. Location of thermocouples in stator disks.

fixing, a small hole or depression is made to house the thermocouple bead. The space is later filled with M-seal, which is thermally conductive. The rotor thermocouples, after fixing, are brought to the end of the shaft through the holes drilled in the Hylam disk and are finally connected to the slip-ring mechanism. The stator thermocouples are brought out radially and connected to the digital mullivoltmeter through a selector switch. The reference temperature is taken as that of the ambient air, which is measured by a mercury-in-glass thermometer of 0.05°C accuracy. The emf reading of every thermocouple is corrected according to the reference temperature.

The slip-ring assembly of 24 rings has gold-plated contacts to ensure minimum contact drop. The slip ring exhibits low noise in the microvolt range even at high speeds. Though measurements are taken only up to 1000 rpm, the slip-ring assembly is capable of handling speeds up to 15,000 rpm. A Hylam disk is fixed on the shaft as the junction box, on which a number of terminals are fixed. The thermocouples from the rotor and the lead wires from the slip-ring assembly are connected to these terminals. While the positive terminals of the thermocouples are connected individually to a terminal of the Hylam disk, all the negative terminals of the rotor thermocouples are shorted and connected to one terminal of the

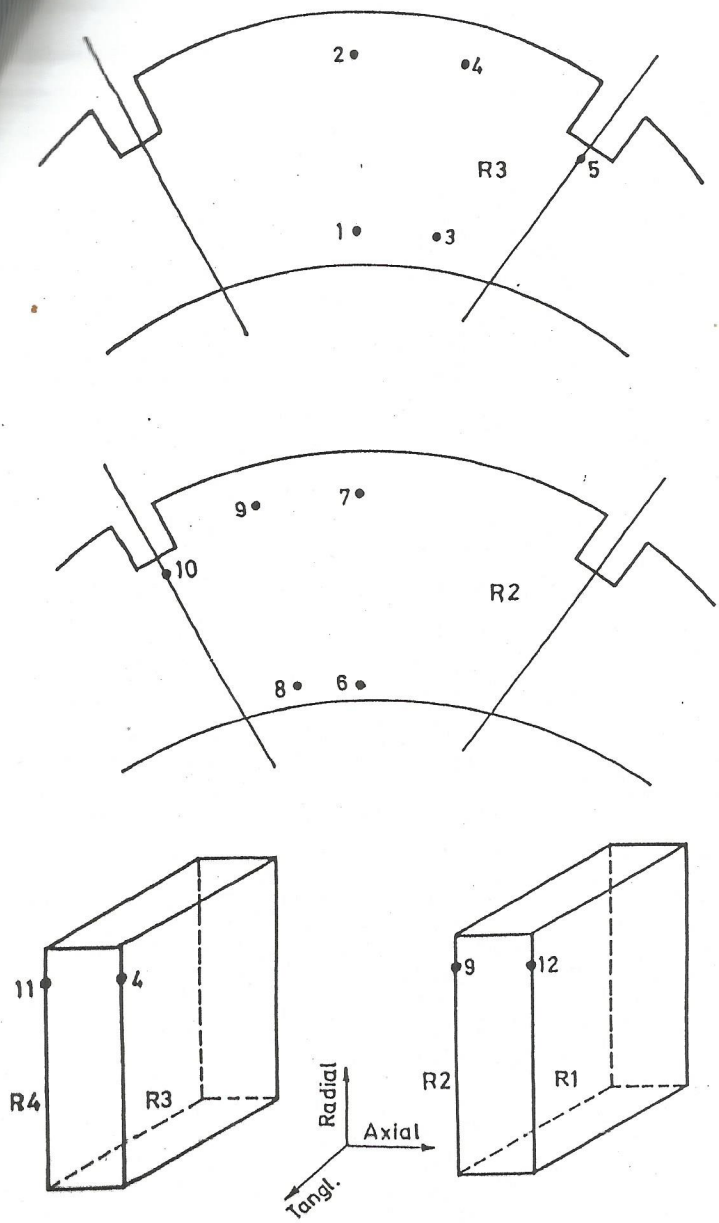

Figure 6. Location of thermocouples in rotor disks.

Hylam disk. This facilitates measurement of temperature of 23 rotating points on the rotor with the available slip-ring assembly.

The air thermocouples in the rotor radial duct are fixed through axial holes drilled in one of the disks. The thermocouples project axially out of the disks in such a way that the bead is at the axial center of the radial duct. Care is taken to prevent sagging of the thermocouples.

The rotor shaft and the rotating member of the slip-ring assembly are mechanically coupled by a flexible metallic hose. Each slip ring has two brushes to ensure definite contact. The output through the brushes is measured by a digital millivoltmeter through a selector switch.

To start with, the experimental setup is run at different speeds without any heating of the disks; the disks are kept at ambient temperature. These initial runs are made to allow for bedding of the brushes and to check for spurious voltages that may be generated by frictional heating of the slip rings and brushes. Temperatures are measured at several points in the rotor and stator disk surfaces. They are found to be equal and identical to the ambient temperature, thus ensuring that no spurious emf is being generated in the temperature-measurement circuit.

EXPERIMENTAL RESULTS AND DISCUSSIONS

Experiments are carried out for the following operating conditions: Re = 1825–3850 for the rotor and a corresponding Re = 1150–2450 for the stator. The correspondence of the rotor and stator Reynolds numbers is based on the same mass

flow rate. Speed of rotation of the rotor is varied from 0 to 700 rpm, which corresponds to a Taylor number range of 0–102. The experiments are repeated for different stator/rotor heat inputs such as 600/300, 800/400/ and 1000/500 W.

The heat transfer coefficient is defined on the basis of logarithmic mean temperature difference, assuming fully developed flow for most of the passage length:

$$h = Q \ln \frac{[T_{w,\text{out}} - T_{c,\text{out}})/(T_{w,\text{in}} - T_{c,\text{in}})]}{A[T_{w,\text{out}} - T_{c,\text{out}}) - (T_{w,\text{in}} - T_{c,\text{in}})]} \quad (1)$$

where

$$T_{w,\text{in}} = (T_{10} + T_{14} + T_5 + T_1)/4 \quad \text{for stator (Fig. 6)}$$
$$= (T_8 + T_6 + T_1 + T_3)/4 \quad \text{for rotor (Fig. 7)}$$
$$T_{w,\text{out}} = (T_{13} + T_{17} + T_8 + T_4)/4 \quad \text{for stator (Fig. 6)}$$
$$= (T_9 + T_7 + T_2 + T_4)/4 \quad \text{for rotor (Fig. 7)}$$

$T_{w,\text{in}}$ and $T_{w,\text{out}}$ are measured on the disk wall surfaces at the same radial location as $T_{c,\text{in}}$ and $T_{c,\text{out}}$, respectively. The location thermocouples for measurement air temperatures $T_{c,\text{in}}$ and $T_{c,\text{out}}$ are indicated in Fig. 5.

The Taylor number (Ta), based on disk spacing, is defined as

$$\text{Ta} = B^2\Omega/\nu \quad (2)$$

The heat transfer performance is expressed in terms of the Nusselt number, and plots are made against Re and Ta for different heat inputs. For heat transfer calculations, all the physical properties of air are evaluated at the arithmetic mean of the temperatures of air at the inlet and exit of the core.

The Nusselt number is defined in terms of the disk spacing as

$$\text{Nu} = hD_H/k \quad (3)$$

Figures 7–12 show the variation of Nu plotted against Re for various Taylor numbers, for both the stator and the rotor. Although the stator is not rotating, the graphs indicate the influence of the rotation of the rotor on the stator heat transfer augmentation. It is seen from Figs. 7, 9, and 11 that the Nusselt number for the rotor radial duct increases monotonically with increase in Re. The value of Nu at the upper limit of Re is almost double its value at the lower limit of Re, for the range of Re considered. Whereas Figs. 8, 10, and 12 indicate considerable increase in stator heat transfer with increase in Re, the effect appears to reach a maximum at the maximum Re investigated. However, more data are required to confirm this trend.

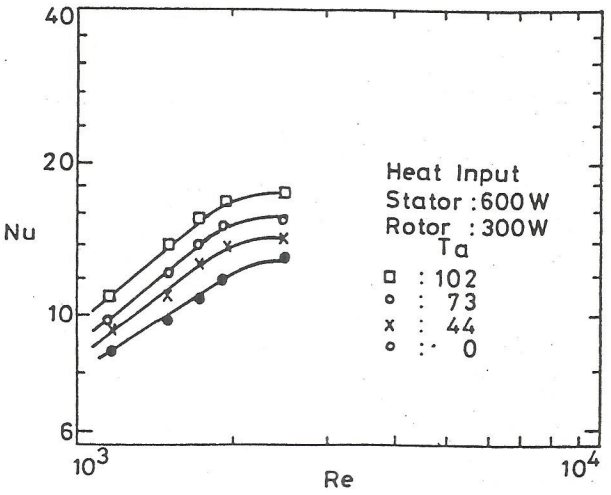

Figure 8. Nu versus Re for stator radial duct at different Ta.

In order to find the Nusselt number for the no-flow condition (Re = O) for different Taylor numbers, the graphs, when extended to intercept the ordinate (Figs. 14 and 15), show good agreement with work carried at earlier for no-flow situations [7], thus establishing the reliability of the present investigation.

Figures 7, 9, and 11 show that at an Re value of about 3000 the Nusselt number appears to increase sharply with Re. As pointed out in Ref. 4, this is attributed to the onset of transition at a Reynolds number of about 3000. Furthermore, the flow goes through different regimes of transition from laminar, through oscillating, to turbulent flow. Similar behavior, though to a much milder extent, is evident for the stator heat transfer coefficient.

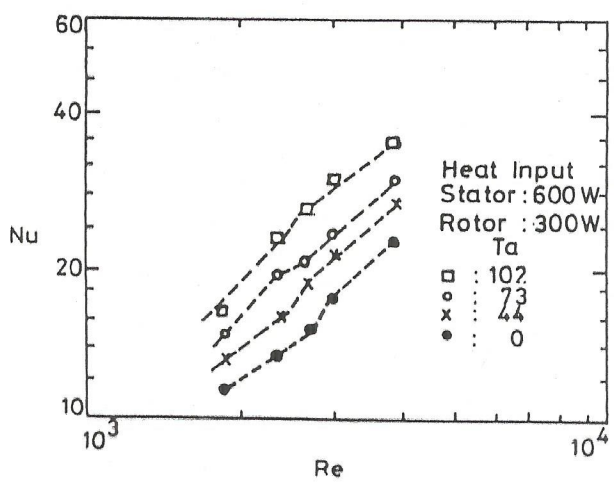

Figure 7. Nu versus Re for rotor radial duct at different Ta.

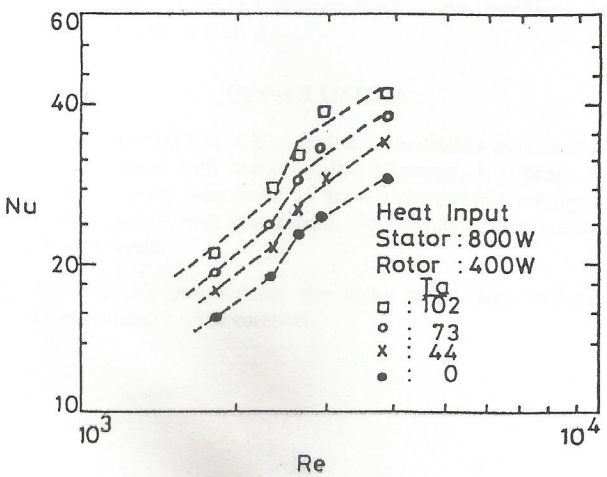

Figure 9. Nu versus Re for rotor radial duct at different Ta.

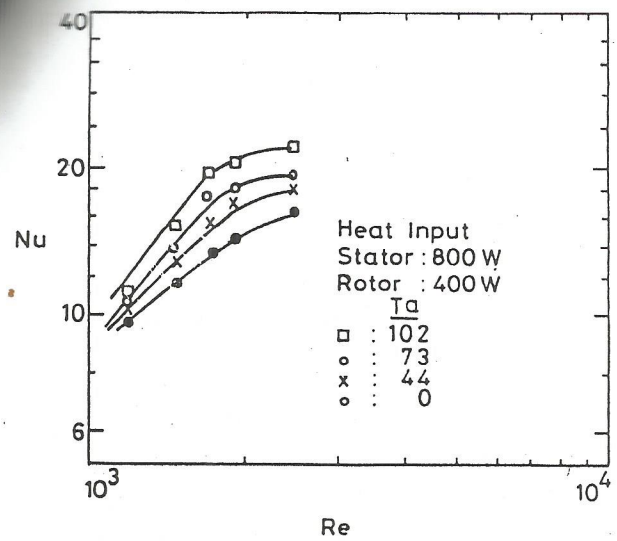

Figure 10. Nu versus Re for stator radial duct at different Ta.

To study the effect of Taylor number values more clearly, Fig. 16 represents a cross plot of Nu against Ta for various Re values and a particular heating condition. The continuous increase of Nu with increasing Ta is not only well marked in the rotor but also significant in the stator, indicating the effect of centrifugal forces on the air particles and the inertial forces. Similar trends are observed at other test runs simulating different heating conditions.

Figure 17 shows the variation of Nu with Ta for a given Re and various heating conditions. The values are higher at higher heat losses, indicating that at higher heat losses, higher temperature will set in free convection currents leading to forced convection and hence higher Nu values. The same trend has been observed at other Reynolds numbers.

No information is available in the literature for such a rotor-stator combination as the present work. The earlier studies concentrated on rotor heat transfer with the rotor open to the ambient atmosphere, whereas in the present test configuration, parallel concentric stationary disks enclose the rotor disks. This renders the present investigation difficult insofar as comparison of test result is concerned. However, the present result is compared with some earlier data [8, 9, 10] for the no-rotation case in Fig. 18. As an additional check, a resistance network for the test section was made, and the experimentally obtained values of the heat transfer coefficients were used to calculate the convective resistances of the network. The temperature distribution in the disks obtained by the network method agreed well with the experimentally measured values (Fig. 13). It is estimated from heat loss calculations that the error may be of the order of 10–20%.

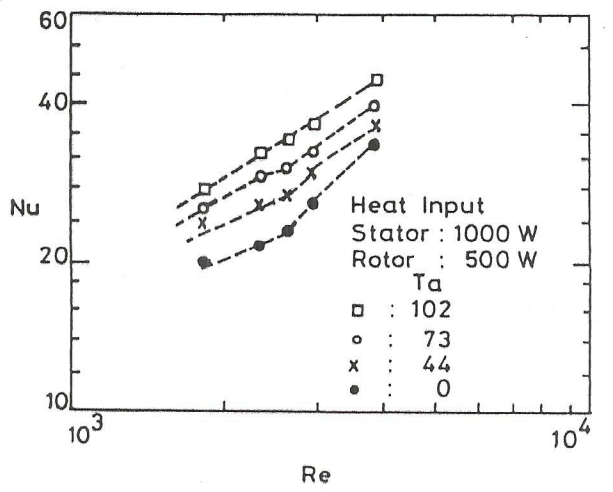

Figure 11. Nu versus Re for rotor radial duct at different Ta.

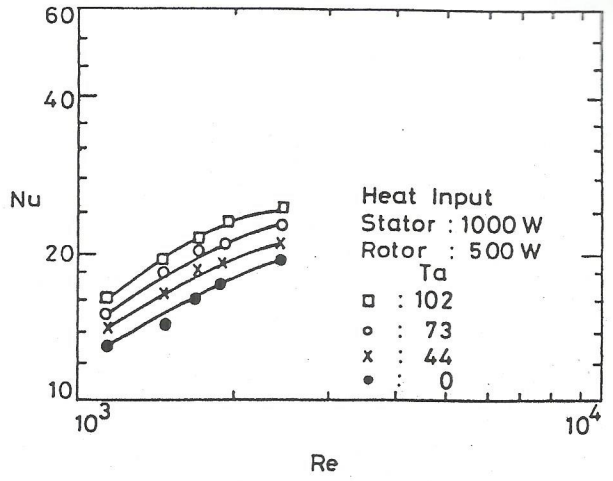

Figure 12. Nu versus Re for stator radial duct at different Ta.

PRACTICAL SIGNIFICANCE AND USEFULNESS OF THE RESULTS

The heat transfer coefficients determined with rotating disks are found to be higher than those with stationary disks. The heat transfer coefficient values can be used in the calculation of convective thermal resistances. Together with conductive thermal resistances they can be used in forming a thermal network for an electric machine, the solution of which gives the temperature distribution in the machine. The heat transfer coefficient values of the present work were used in this manner, and the temperatures in an actual 600 kW induction motor were predicted. The predicted values compared satisfactorily with the measured temperatures in the machine. The details are given in Ref. 11.

CONCLUSION

The experimental setup is a realistic simulation of a rotating electric machine with radial cooling channels. It appears that no previous work was done on such a rotor-stator configuration with internal heat generation. The results can be summarized as follows:

1. The Nusselt number for the rotor radial duct increases monotonically with rotation.

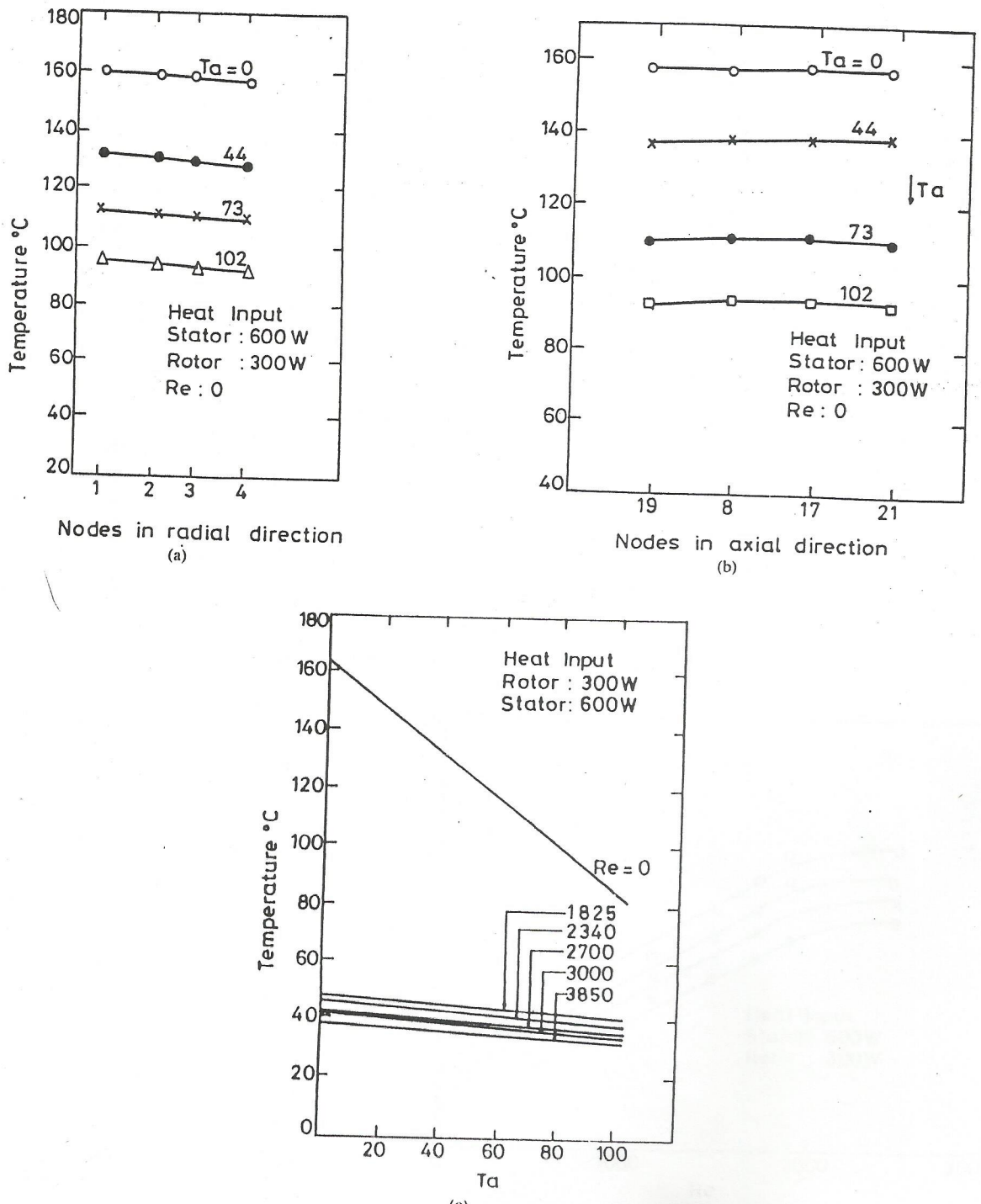

Figure 13. (*a*) Radial temperature distribution of stator disks for various Ta and a given Q (Fig. 5). (*b*) Axial temperature distribution of rotor disks for Re = 0 with varying Ta and given Q (Fig. 6). (*c*) Variation of a typical rotor node temperature with Ta for different Re and given Q.

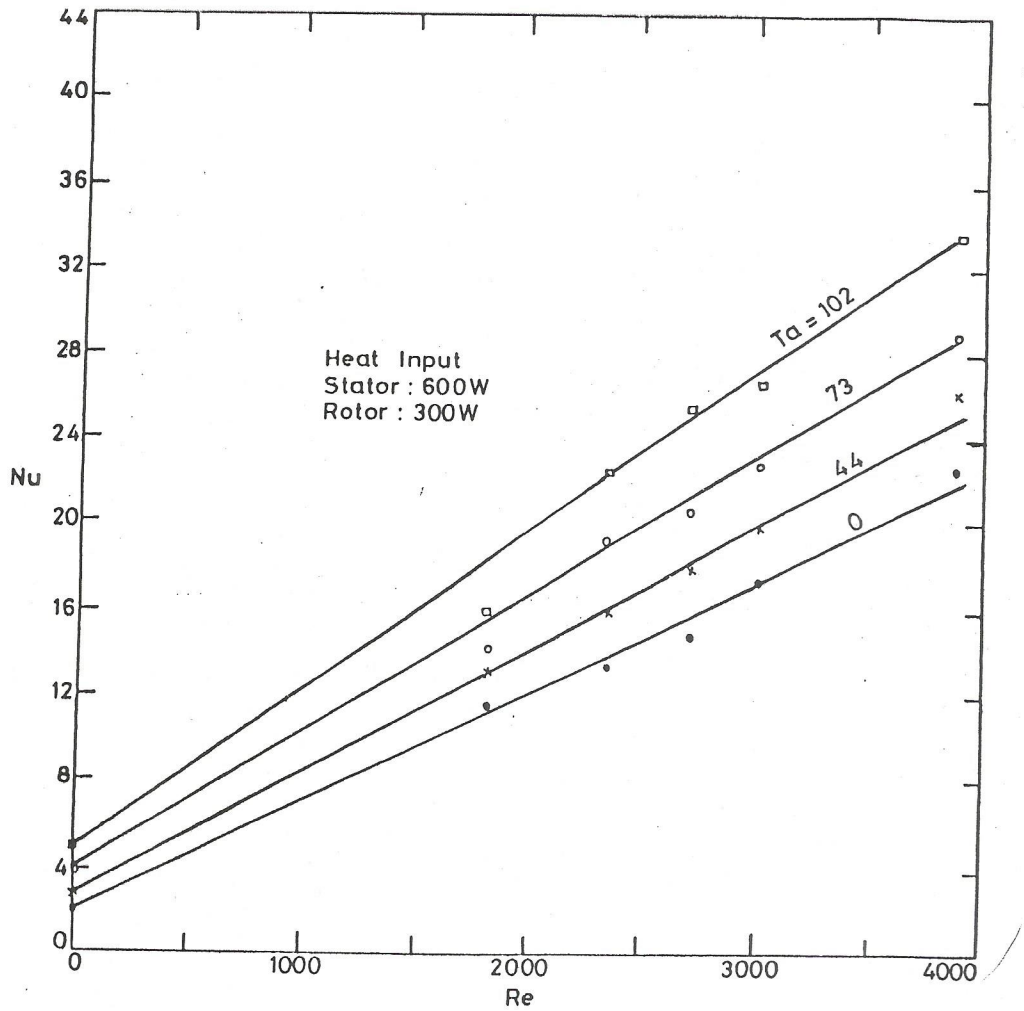

Figure 14. Variation of Nu in rotor radial duct with Re for different Ta.

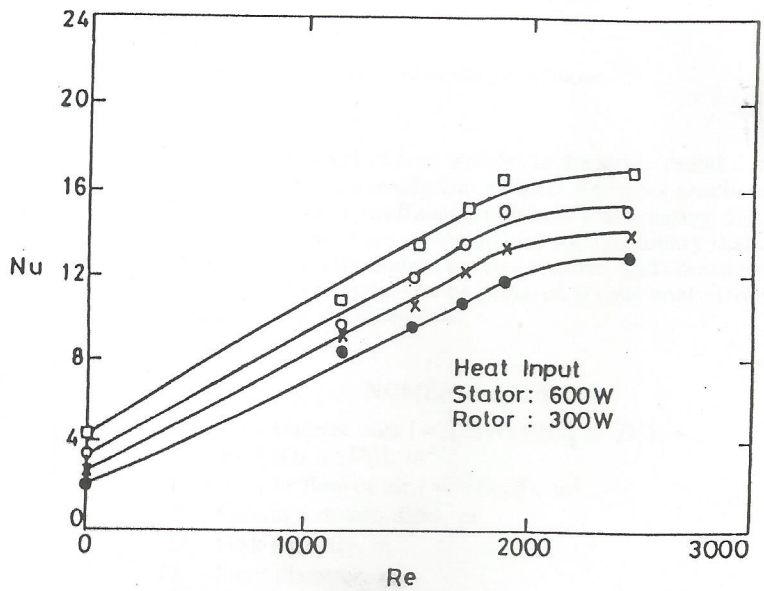

Figure 15. Variation of Nu in stator radial duct with Re for different rotor Ta.

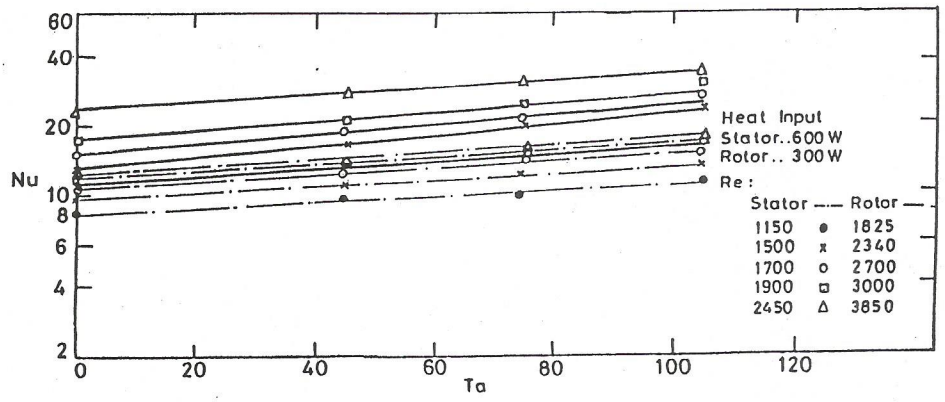

Figure 16. Variation of Nu in rotor and stator radial ducts with Ta for different Re.

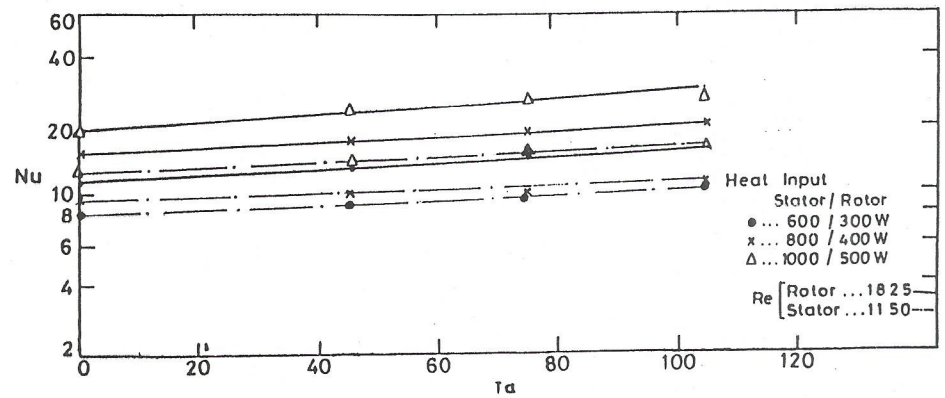

Figure 17. Variation of Nu in rotor and stator radial ducts with Ta for different heating conditions.

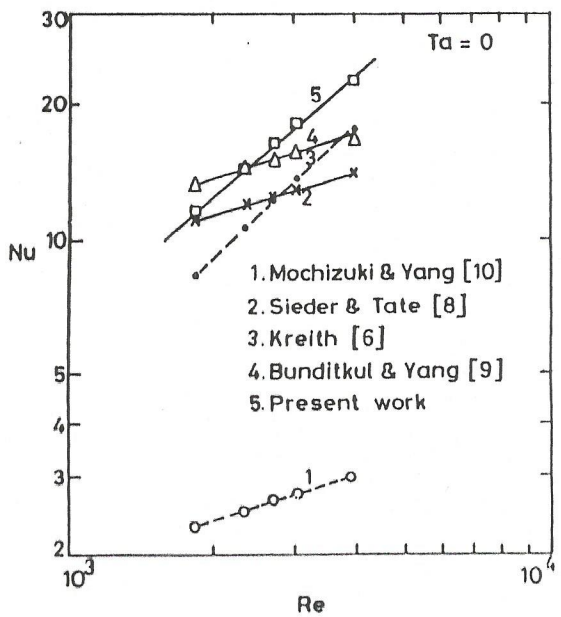

Figure 18. Comparison of present work.

2. The augmentation of heat transfer in the stator radial duct appears to reach a maximum at higher Reynolds numbers.
3. The heat transfer coefficients obtained with rotating disks are much higher than those obtained with stationary disks. Hence present-day designs are conservative, and considerable saving in material can be achieved if rotational effects are taken into consideration.

NOMENCLATURE

A	Heat transfer area [$= (2\pi N/4)(D_2^2 - D_1^2) + \pi NL(D_2 + D_1)$], m^2
A_c	Area of flow of air ($= \pi D_m B$), m^2
B	Spacing between disks, m
D	Disk diameter, m
D_1	Inner diameter, m
D_2	Outer diameter, m
D_H	Hydraulic diameter ($= 2B$), m
D_m	Mean diameter, m
G	Mass velocity ($= m/A_c$), kg/(m^2 s)
h	Average heat transfer coefficient, W/(m^2 K)
k	Thermal conductivity of air, W/(m K)
L	Axial dimension of disks, m

- Mass flow rate of air, kg/s
- Number of disks
- Nusselt number (= hD_H/k), dimensionless
- Rotational speed of rotor, rps
- Q Heat input, W
- Re Reynolds number (= GD_H/μ), dimensionless
- T Temperature, °C
- Ta Taylor number (= $B^2\Omega/\nu$),

Greek Symbols

- Ω Angular velocity of rotor (= $2\pi n$), rad/s
- ν Kinematic viscosity of air, m^2/s
- μ Dynamic viscosity of air, kg/ms

Subscripts

- w Wall
- c Cold fluid
- R Rotor
- S Stator

REFERENCES

1. Weedy, B. M., The Determination of Transient Temperature Distribution in a Turbo-Alternator Rotor by an Analogue, IEE Monograph No. 4725, 190 (c), pp. 126–137, 1961.
2. Nonaka, S., Yamamoto, M., Nakano, M., and Kawase, M., Analysis of Ventilation and Cooling System for Induction Motors, *Trans. IEEE,* **PAS-100**, 4636–4643, 1981.
3. Subba Rao, B. K., Heat Transfer from Partially Enclosed Disks Rotating in Air with Uniform Wall Heat Flux, *Indian J. Technol.,* **15**, 177–184, 1977.
4. Mochizuki, S., Yang, W. J., Yagi, Y., and Ueno, M., Heat Transfer Mechanisms and Performance in Multiple Parallel Disk Assemblies, *ASME J. Heat Transfer,* **105**, 598–604, 1983.
5. Sim, Y. S., and Yang, W.-J., Numerical Study on Heat Transfer in Laminar Flow through Corotating Parallel Disks, *Int. J. Heat Mass Transfer,* **27**, 1963–1969, 1984.
6. Kreith, F., Transfet de Chaleur et de Masse dans un Ecoulement Radial entre Deux Disques Paralleles Fixes ou Tourant a la meme Vitesse, *Int. J. Heat Mass Transfer,* **9**, 265–282, 1966.
7. Banerjee, B., Rao, K. V. C., and Sastri, V. M. K., Transient Free Convective Heat Transfer from Corotating Concentric Disks, accepted for publication in IJHMT.
8. Sieder, E. N., and Tate, G. E., Heat Transfer and Pressure Drop of Liquids in Tubes, *Ind. Eng. Chem.,* **28**, 1429, 1936.
9. Bunditkul, S., and Yang, W.-J., Laminar Transport Phenomena in Parallel Channels with a Short Flow Constriction, *ASME J. Heat Transfer,* **101**, pp. 217–221, 1979.
10. Mochizuki, S., and Yang, W.-J., Heat Transfer and Friction Loss in Laminar Radial Flows through Rotating Annular Disks, *Trans. ASME J. Heat Transfer,* **103**, 212–217, 1981.
11. Banerjee, B., Analogue and Experimental Heat Transfer Studies on Simulated Rotating Electrical Machines, Ph.D. Thesis, Dept. of Mechanical Engineering, Indian Inst. Tech., Madras, 1987.